

Thermal barrier coatings on laser surface modified AISI H13 tool steel using Atmospheric Plasma Spray Technique

M. S. Reza^{1, a}, S. N. Aqida^{1, b}, Mohd Radzi Mohd Toff^{2, c} and D. Brabazon^{3, d}

¹Faculty of Mechanical Engineering, Universiti Malaysia Pahang, 26600 Pekan, Pahang, Malaysia

²Advanced Materials Research Centre, Sirim Berhad, Lot 34, Jalan Hi-Tech 2/3, KULIM HI-TECH PART, 09000 Kulim, Kedah, Malaysia

³Advanced Processing Technology Research Centre, Dublin City University, Dublin 9, Ireland

^amdreza@ump.edu.my, ^baqida@ump.edu.my, ^cmradzit@sirim.my, ^ddermot.brabazon@dcu.ie

Keywords: AISI H13 steels, thermal barrier coatings, Ytria Stabilized Zirconia, NiCrAlY,

Abstract: This paper presents yttria-stabilized zirconia (YSZ) coating deposition on laser surface modified H13 tool steel using atmospheric plasma spray (APS) technique. A Praxair Plasma Spray System with SG-100 gun was used to deposit coating materials on laser-modified H13 tool steel substrate surface. A bond coat layer material was NiCrAlY alloy while the top coat was yttria stabilized zirconia (YSZ) with powder size distribution range of -106 μm to +45 μm . A 2³ design of experiment (DOE) was used to deposit bond coat and top coat powders with three controlled factors of input current, powder feed rate and stand-off-distance. The design was optimised for minimum porosity and maximum hardness. The coating thickness and percentage of porosity were measured using IM7000 inverted optical microscope. Hardness properties of top coating layer were measured by using MMT-X7 Matsuzawa Hardness Tester Machine with vickers hardness scale. The microscopy findings indicated variations of coating thickness at different parameters settings. Samples at the highest current and powder feed rate and lowest stand-off distance settings produced a lower porosity percentage and higher hardness. A higher powder feed rate with the smallest stand-off-distance allowed melted powders to travel uniformly onto the substrate surface. These findings were significant to development of thermal barrier coatings on semi-solid forming die surface.

Introduction

In forming applications, die surface was rapidly heated during molten metal injection, and was cooled by water quenching during solidification [1]. Repetitive cycles of these processes initiated premature failure in dies such as thermal fatigue (heat checking), erosion, corrosion, local adherence of the casting alloy to the tool (soldering) and gross fracture [2, 3, 4]. Erosion is physical impingement of incoming liquid and partially solid alloy onto die surface.

Thermal spray processes like flame spray, electric arc spray, and plasma arc spray have been used to deposit metallic or non-metallic coatings [5, 6]. For thermal barrier coating application, YSZ in powder form was heated to a molten state or semi molten state and was projected in the form of micrometer size particles at high speed onto substrate surface using atmospheric plasma spray. Coating quality was determined by its porosity content and hardness properties [7, 8]. Though much works have been conducted on porosity study in thermal spray coatings, and effects of micro-cracks and pores on coating properties, limited works reported on atmospheric plasma spray parameters effects on porosity content in YSZ coating [9, 10-13].

Several attempts have been carried out to establish relationship of thermal spray coating process parameters such as Taguchi method, full and fractional DOE [14,15]. A full factorial design with three factors and two levels was reported to determine the dependence of photocatalytic activity of titania coatings on plasma power, carrier gas flow rate, and powder feed rate [16].

Generally, both hardness and porosity content were related where coating with high content porosity produced varied hardness properties [17]. Excessive porosity content influenced structural integrity of coating. During plasma spraying process, pores can be generated from entrapped gases, incomplete filling and shrinking during rapid solidification of splats. Major problems in plasma sprayed coatings were presence of open pores, closed pores and micro-cracks which reduced mechanical properties of coating such as elastic modulus, micro-hardness and bonding strength [18]. Porosity varied from 2% to more than 20% which dependent to spray parameters. Changes of spray parameters influenced particle velocity and temperature which were closely linked to coating hardness and porosity content [14]. The porosity of plasma-sprayed coatings was analysed using digital image analysis [19]. In this study, experimental techniques have been utilised to study erosion failure mechanism that related to the coating density. Low erosion failure may occur with low porosity and high hardness obtained.

Methodology and materials

AISI H13 steel was used as substrate material and chemical composition of the substrate materials is given in Table 1. Bond coat powder used was Praxair Nickel based NiCrAlY (Ni-164/211 Ni 22%Cr 10%Al 1.0%Y) while top coat, Praxair Ai-1075 ceramic coating yttria stabilized zirconia ($ZrO_2 + 8 \text{ wt.}\% Y_2O_3$).

Samples of 10 mm diameter and 150 mm length were processed using CO_2 laser system with range of treated surface thickness of 10 to 32 μm . Details of processing was as described elsewhere [ref]. The laser modified sample was coated using APS method with parameters given in Table 2. Sample was rotated by controllable speed chuck during deposition and was positioned at a stand-off distance perpendicular to robotic arm which held plasma spray gun. The robotic arm was translated in z-direction to deposit the entire sample surface. In Table 2, bond coat was deposited at constant feed rate, stand-off distance and current while top coat processing was conducted at 2^3 design of experiment. The parameters settings for 2^3 DOE is shown in Table 3.

Metallographic study was conducted using IM7000 inverted optical microscope. Samples were measured for hardness using MMT-X7 Matsuzawa Hardness Tester Machine with vickers hardness scale while porosity content was analysed using ImageJ software.

Table 1: Chemical composition of AISI H13 steel (wt. %)

Material	C	Mn	Si	Cr	Ni	Mo	V	Cu	P	S	Fe
H13	0.32- 0.45	0.20- 0.50	0.80- 1.20	4.75- 5.50	0.30	1.10- 1.75	0.80- 1.20	0.25	0.03	0.03	Bal.

Table 2: Praxair plasma spray system parameter settings

Parameters	Unit	Bond coat (NiCrAlY) setting	Top coat (YSZ) setting	
Secondary gas (He)	kPa	345	827	
Primary gas (Ar)	kPa	345	345	
Carrier gas (Ar)	kPa	345	207	
Workpiece rotational speed	rpm	250	250	
No. of cycle	no.	4	22	
Torch speed	%	5	5	
Input Current	Ampere	550	550	650
Feed Rate	g/min	29.8	36.3	51.7
Stand-off distance	mm	110	100	120

Table 3: DOE 2³ level parameter settings

Sample no.	Current, A	Feed rate, g/min	Stand-off distance, mm
1	550	51.7	120
2	650	36.3	120
3	650	36.3	100
4	550	51.7	100
5	650	51.7	100
6	550	36.3	120
7	550	36.3	100
8	650	51.7	120

Results and discussions

Micrograph in Figure 1 shows an example cross-sectional area of coated sample obtained. The sample cross-section consists of YSZ coating layer [A], NiCrAl alloy coating [B], laser modified layer [C] and substrate material [D]. Range of coating layers thickness is given in Table 4, where bond coat and top coat thickness varied from 145 to 225 μm , and 100 to 550 μm respectively. The highest range was measured in sample 5 which was processed at higher input current, 650 A, higher feed rate, 51.7 g/min and minimum stand-off distance, 100 mm. Sample 1 produced the lowest range of top coating thickness of 100 to 170 μm .

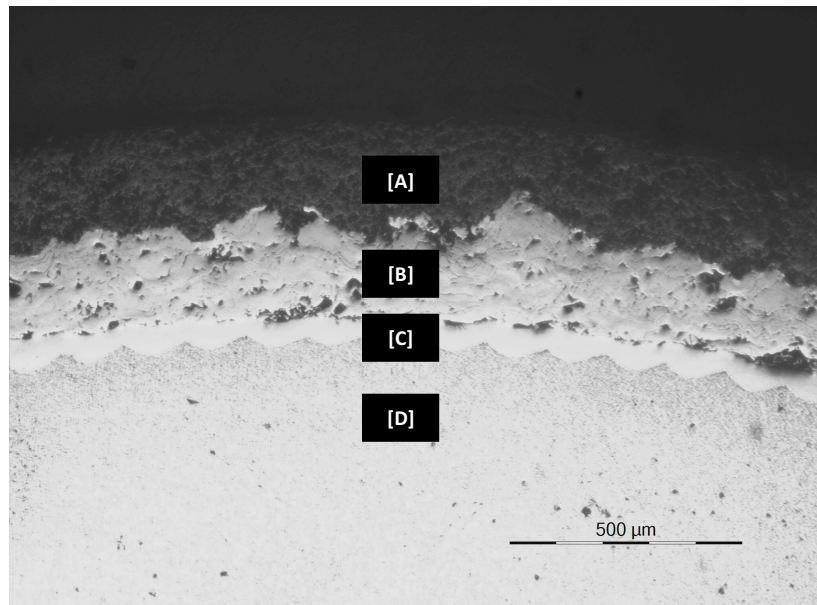


Figure 1: Micrograph of cross-sectional surface of coated laser modified sample

The coating layers consist of porosity formation as shown by micrographs of Figure 2. High distribution of porosity in the top coat layer is shown in Figure 2(a) while low porosity distribution is given in Figure 2(b). Porosity content in both coating layers of each sample is shown by Figure 3. Porosity percentage in top coat varied with parameter settings. The lowest porosity percentage of 41% in top coat was measured from sample 5 which was deposited at higher input current, 650 A, higher feed rate, 51.7 g/min and lower stand-off distance, 100 mm. The highest porosity of 63% was analyzed in sample 6 which was coated at lower input current, 550 A, lower feed rate, 36.3 g/min and higher stand-off distance, 120 mm. In bond coat layer, the porosity content was in the range of 3 to 18%.

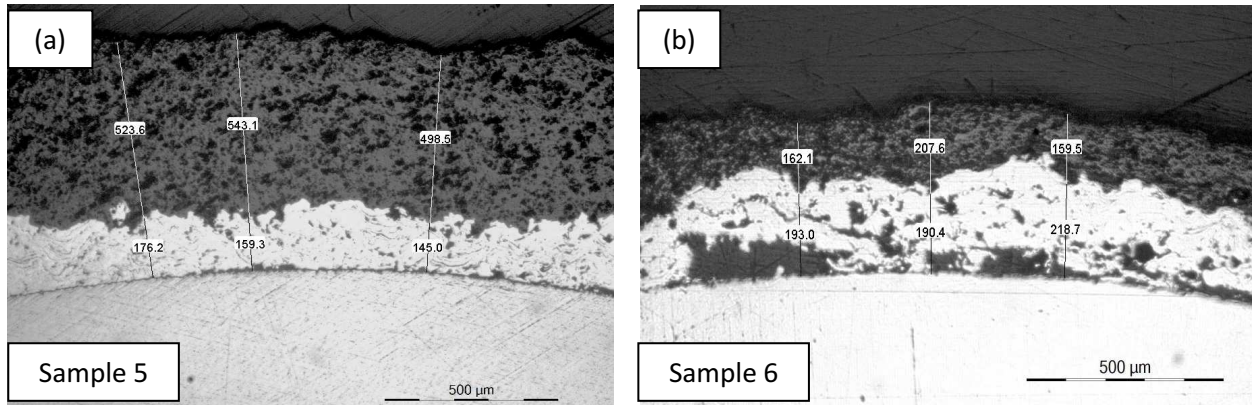


Figure 2: Micrograph of YSZ and NiCrAlY coatings on laser modified H13 tool steel in (a) sample 5 and (b) sample 6

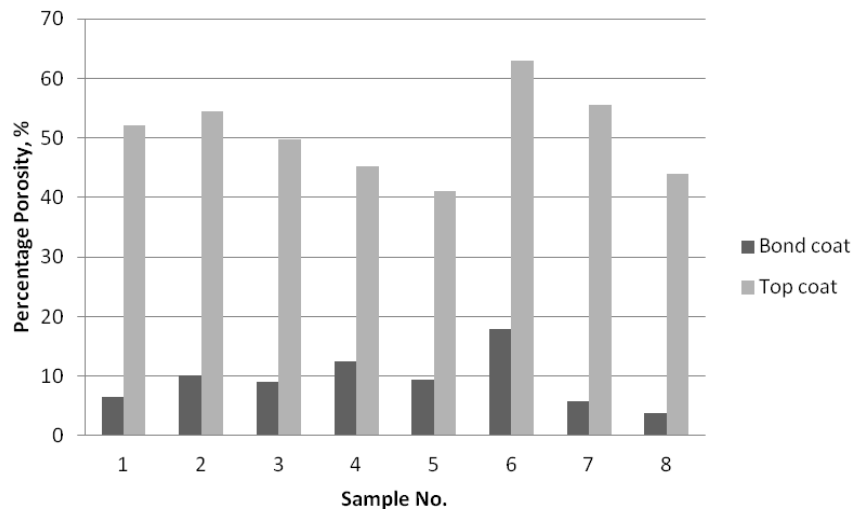


Figure 3: Porosity content in coating layers of laser modified AISI H13 samples

Porosity formation was affected by input current, powder feed rate and stand-off distance setting. Experimental using atmospheric plasma spray (APS) produced an amount of heat energy to melt the coating powder which was called enthalpy. A higher input current of 650 A in sample 5 produced more efficient deposition where a higher heat energy in the plasma leads to a better in-flight particle molten state [12]. Thus, the particle flow was enhanced and viscosity was decreased. This phenomenon resulted in a uniform distribution of coating layer on the substrate. Besides, with lower stand-off distance settings in sample 5, the enthalpy of the molten ceramic particles was largely stored without having lost tremendously during coating process. The particles maintained their molten state because of short travelling distance of the particles to the substrate. Under this condition, the molten particles deposited overlapping layers on the substrate surface, thus resulted in low percentage of porosity in the coating.

In sample 6, porosity formation was the highest as with lower input current setting. Insufficient amount of energy for in-flight molten state particles causing non-uniform coating deposition onto substrate. With higher stand-off distance, molten material solidified faster due to heat loss upon compaction. A low powder feed rate of 4 g/min decreased deposition efficiency due to particles vaporization to the surrounding air.

An increase in porosity will lower the coating stiffness. Despite of high input current is good to decrease the percentage amount of porosity, too high arc current settings, may decrease the coating deposition efficiency. A thin cap gas bubbles leaving behind a residual hole on the coating surface will increase the percentage amount of porosity. This is because very high arc current settings needs a very high gas pressure in the gas layer prior to impact. Consequences of this, the gas escape resulting in escalating gas pressure in the splat centre during rapid spreading and quenching of splats. Extremely very high arc current settings may result in vaporization of particles [17].

Range of coating thickness on laser surface modified samples for bond coat and top coat was shown in Table 4.

Table 4: Range coating thickness on laser surface modified samples

Sample	Range of thickness (μm)	
	Bond coat (NiCrAlY)	Top coat (YSZ)
1	180 - 225	100 - 170
2	170 - 200	260 - 290
3	173 - 180	460 - 500
4	145 - 165	300 - 320
5	145 - 180	500 - 550
6	190 - 220	150 - 220
7	200 - 220	200 - 220
8	180 - 230	330 - 350

At constant parameter settings, variation of bond coat layer thickness was possibly due to small misalignment of sample rotation. In top coat layer, the higher range of thickness in sample 5 was due to higher input current setting of 650 A. Higher energy in the plasma leads to a better and uniform coating deposition efficiency.

The lower coating thickness range in sample 1 was due to the higher feed rate setting which increased the amount of particles to share the kinetic energy. Thus, particles velocity and thermal energy of the plasma flame decreased.

Hardness of coated laser modified H13 is shown in Figure 4. The top coat layer hardness range of 150 to 550 HV_{0.1} was measured at 120 μm depth from sample surface, while the bond coat layer hardness of 280 HV_{0.1} was measured at 670 μm depth. The highest hardness range was measured across sample 5 cross-section. In sample 5, the top coat layer exhibited 400 HV_{0.1} hardness. A lower hardness of 300 and 150 HV_{0.1} was measured in sample 3 and 6 respectively. The bond coat layer hardness in the samples was between 270 and 290 HV_{0.1}.

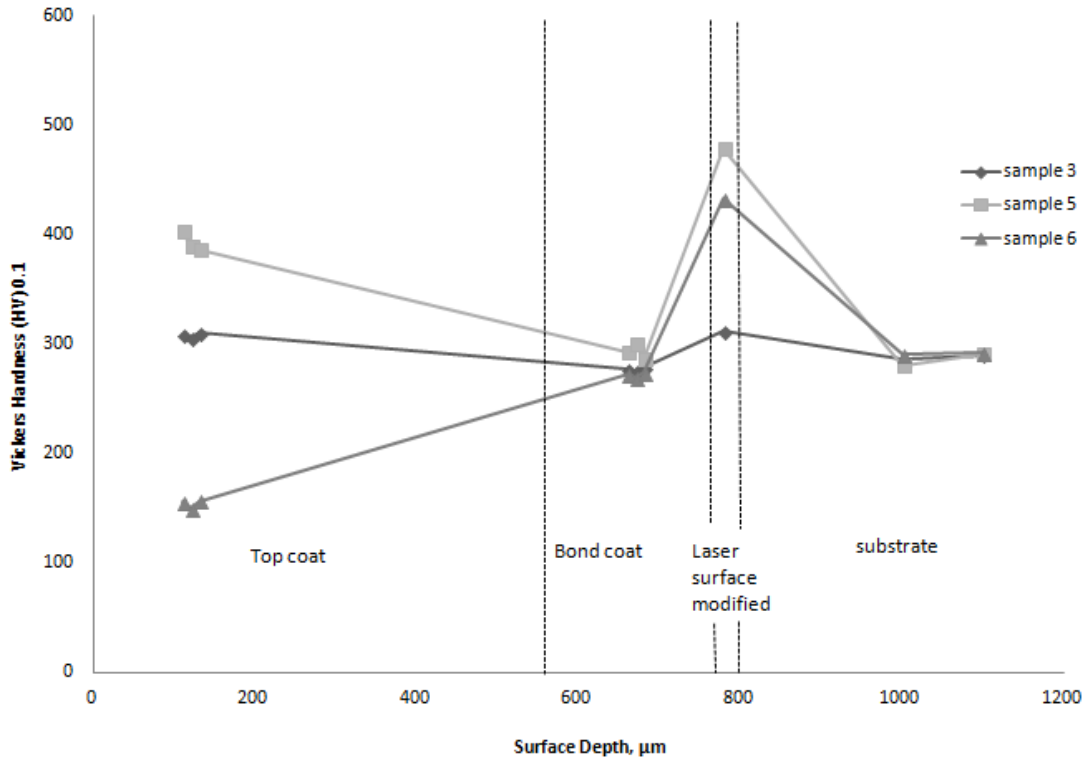


Figure 4: Hardness of cross-sectional surface of coated laser modified H13 steel substrate

The highest hardness properties achieved in top coating of sample 5 was due to low porosity content of the coating and the lowest hardness properties measured in sample 6 was resulted from high porosity content. Referring to porosity content in sample 6, pores formation within the molten layer during solidification altered the coating layer integrity. Lower input current and feedrate along with high stand-off distance settings decrease particles flattening ratio upon coating deposition. Whereby, for sample 5, higher input current and feedrate with low stand-off distance settings the fully molten particles deposited overlapping layers were fully flattened contributes to low porosity percentage. A gradient of hardness properties across the substrate signifies its relationship with coating mechanical properties. Presence of open pores, closed pores and micro-cracks reduced coating hardness along with reduced mechanical properties of coating such as elastic modulus, micro-hardness and bonding strength [18].

Conclusion

Higher settings of input current, 650 A and feed rate, 51.7 g/min along with lower setting of stand-off distance, 100 mm have significant effect on the microscopy findings of coating thickness, coating porosity and hardness. Higher input current setting assist in increasing the thermal energy during APS coating. While, feed rate supply the sufficient amount of powder for efficient coating deposition. Low stand-off distance maintain the particles enthalpy by reducing molten particles heat loss to surrounding air.

Acknowledgement

This work was supported by Universiti Malaysia Pahang and Fundamental Research Grant Scheme-RDU120105 from Ministry of Higher Education Malaysia.

References

- [1] Amit Srivastava, Vivek Joshi, Rajiv Shivpuri, Rabi Bhattacharya, Satish Dixit, A multilayer coating architecture to reduce heat checking of die surfaces, *Surface and Coatings Technology*, Volumes 163–164, 30 January 2003, Pages 631-636, ISSN 0257-8972, 10.1016/S0257-8972(02)00690-4.
- [2] L.J.D. Sully, in "Metals Handbook, 9th ed., vol. 15" (ASMInternational, Metals Park, Ohio, 1988) p. 286.
- [3] J.R. Davis (Ed.), in "ASMSpeciality Handbook, Tool Materials" (ASMInternational, Materials Park, Ohio, 1995) p. 251.
- [4] D.F. ALLSOP, D. KENNEDY, in "Pressure diecasting, Part 2: The technology of the casting and the die" (Pergamon Press Ltd, Oxford, 1983).
- [5] JR Davis, Introduction to Thermal Spray Processing, *Handbook of Thermal Spray Technologies*, ed., ASM International, Materials Park, OH, p. 3–9, 2004.
- [6] R.C. Tucker, Jr., Thermal Spray Coatings, *Surface Engineering*, Vol 5, *ASM Handbook*, ASM International, 1994, p 497–509.
- [7] A. Abdellah El-Hadj, M. Zirari, N. Bacha, Numerical analysis of the effect of the gas temperature on splat formation during thermal spray process, *Applied Surface Science*, Volume 257, Issue 5, 15 December 2010, Pages 1643-1648, ISSN 0169-4332.
- [8] C.J. Li, A. O hmori, *J. Therm. Spray Technol.*, 11 (2002), p. 365

- [9] L. Wang, J.C. Fang, Z.Y. Zhao, H.P. Zeng, Application of backward propagation network for forecasting hardness and porosity of coatings by plasma spraying, *Surface and Coatings Technology*, 201 (2007), pp. 5085–5089
- [10] X.C. Zhang, B.S. Xu, F.Z. Xuan, H.D. Wang, Y.X. Wu, S.T. Tu, Statistical analyses of porosity variations in plasma-sprayed Ni-based coatings, *Journal of Alloys and Compounds*, 467 (2009), pp. 501–508
- [11] S. Deshpande, A. Kulkarni, S. Sampath, H. Herman, Application of image analysis for characterization of porosity in thermal spray coatings and correlation with small angle neutron scattering, *Surface and Coatings Technology*, 187 (2004), pp. 6–16
- [12] R. Venkataraman, G. Dasa, S.R. Singh, L.C. Pathak, R.N. Ghosha, B. Venkataraman, R. Krishnamurthy, Study on influence of porosity, pore size, spatial and topological distribution of pores on micro-hardness of as plasma sprayed ceramic coatings, *Materials Science and Engineering*, 445 (2007), pp. 269–274
- [13] S. Guessasma, C. Coddet, Neural computation applied to APS spray process: porosity analysis, *Surface and Coatings Technology*, 197 (2005), pp. 85–92
- [14] de Lovelock HL, Villers RPW, Benson JM, Young PM (1998) Parameter study of HP/HVOF deposited WC-Co coatings. *J Thermal Spray Technol* 7(1):97–107.
- [15] Kingswell R, Scott KT, Wassell LL (1993) Optimizing the vacuum plasma spray deposition of metal, ceramic, and cermet coatings using designed experiments. *J Thermal Spray Technol* 2(2):179–186.
- [16] Burlacov I, Jirkovsky J, Muller M, Heimann RB (2006) Induction plasma-sprayed photocatalytically active titania coatings and their characterization by micro-Raman spectroscopy. *Surf Coat Technol* 201:255–264.
- [17] R. Venkataraman, G. Dasa, S.R. Singh, L.C. Pathak, R.N. Ghosha, B. Venkataraman, R. Krishnamurthy, Study on influence of porosity, pore size, spatial and topological distribution of pores on micro-hardness of as plasma sprayed ceramic coatings, *Materials Science and Engineering*, 445 (2007), pp. 269–274
- [18] I.Yu. Konyashin, T.V. Chukalovskaya, A technique for measurement of porosity in protective coatings, *Surface and Coatings Technology*, 88 (1996), pp. 5–11
- [19] Hao Du, Soo Wahn Lee, Jae Heyg Shin, Study on porosity of plasma-sprayed coatings by digital image analysis method, *Journal of Thermal Spray Technology*, 14 (2005), pp. 453–461